American Mineralogist, Volume 78, pages 493–499, 1993

High-pressure crystal chemistry of $KAlSi_3O_8$ hollandite

JINMIN ZHANG
Geophysical Laboratory and Center for High-Pressure Research, Carnegie Institution of Washington, 5251 Broad Branch Road NW, Washington, DC 20015, U.S.A.

JAIDONG KO*
Center for High-Pressure Research, Department of Earth and Space Science, State University of New York, Stony Brook, New York 11794, U.S.A.

ROBERT M. HAZEN, CHARLES T. PREWITT
Geophysical Laboratory and Center for High-Pressure Research, Carnegie Institution of Washington, 5251 Broad Branch Road NW, Washington, DC 20015, U.S.A.

ABSTRACT

A high-pressure single-crystal XRD study of $KAlSi_3O_8$ with the tetragonal hollandite structure has been completed to 4.47 GPa. The *a* axis is approximately twice as compressible as *c*, so *c*/*a* increases with pressure. This anisotropy is similar to that of the structurally related mineral stishovite, though $KAlSi_3O_8$ hollandite is approximately 53% more compressible along both axes. The relative incompressibility of the *c* axis can be explained by the strong cation to cation repulsive forces across the shared octahedral edge in the double chain; Si(Al)-O bonds perpendicular to c are more compressible than those in other directions. *P-V* data give an isothermal bulk modulus of 180(3) GPa using a Birch-Murnaghan equation of state with $K_T' = 4.0$ and constraint of V_0. The polyhedral bulk modulus of the $Si(Al)O_6$ octahedron is 153(9) GPa, the smallest among rutile-related oxides. The KO_8 tetragonal prism has a polyhedral bulk modulus of 181(43) GPa, which is unusually large for an alkali cation site. The volume of the K coordination polyhedron is constrained by the rigid tetragonal octahedral framework, so the bulk modulus is expected to be independent of the size and charge of the central cation.

INTRODUCTION

$KAlSi_3O_8$, which crystallizes as potassium feldspar at near-surface conditions of the Earth's crust, assumes the hollandite structure at much higher pressure and temperature. It may be a common minor phase in the mantle, and, if so, because of the presence of large open tunnels in the structure and its ability to immobilize radioactive elements, it could be a repository of light elements and radioactive elements. In addition, the barium manganese mineral hollandite contains zeolitic H_2O (Gruner, 1943), and much of the H_2O can be retained to at least 500 °C in some species at room pressure (Bish and Post, 1989). Thus, compounds with the hollandite structure may be additional candidates for H_2O storage in the mantle.

Many studies of the structures of hollandite-related compounds have been conducted (e.g., Post et al., 1982; Cheary and Squadrito, 1989; Miura, 1987). The interest lies in the complex problems associated with manganese oxides as well as the role of hollandite in the synthetic rock (Synroc), which contains hollandite as a major phase and has been proposed for use in the storage of radioactive wastes (Ringwood et al., 1979). The structure may adopt either monoclinic or tetragonal symmetry, depending on the ratio of the average ionic radius of the octahedral cations to that of the tunnel cations (Post et al., 1982). High-pressure systematics suggest that the (Si,Al) octahedron and the K tetragonal prism should compress at different rates. Typically, large alkali cation polyhedra are many times more compressible than Si polyhedra (Hazen and Finger, 1982). In the $KAlSi_3O_8$ hollandite structure, however, the volume of the K tetragonal prism is largely constrained by the framework of (Si,Al) octahedra. One would expect that the K site would have a compressibility similar to that of the entire structure, significantly smaller than those of K-O sites without such a constraint.

Ringwood et al. (1967) first synthesized $KAlSi_3O_8$ hollandite and determined the crystal structure using powder film intensity data. A structure refinement was reported by Yamada et al. (1984) using the powder method. An important feature of the structure is that Si is in sixfold coordination—one of the few high-pressure phases so far observed to have $^{[6]}Si$ (Finger and Hazen, 1991). It is indeed one of the only three aluminosilicates known in which Al substitutes for sixfold-coordinated Si, the other two being garnet (Ringwood and Major, 1971) and pe-

* Present address: Department of Ceramic Engineering, College of Engineering, Inha University, 253 Yonghyun-Dong, Nam-Ku, Inchon 402-751, Korea.

0003–004X/93/0506–0493$02.00

Table 1. Unit-cell parameters, axial ratio *c*/*a*, and unit-cell volumes between 0 and 4.47 GPa

P (GPa)	*a* (Å)	*c* (Å)	*c*/*a*	*V* (Å³)
0	9.315(4)	2.723(4)	0.2923(5)	236.26(36)
0.70	9.301(2)	2.719(2)	0.2923(3)	235.15(19)
1.17	9.292(2)	2.717(2)	0.2924(3)	234.59(19)
1.64	9.285(1)	2.717(1)	0.2926(2)	234.19(12)
2.04	9.271(1)	2.714(2)	0.2927(2)	233.30(14)
2.17	9.268(1)	2.713(1)	0.2928(1)	233.06(10)
2.55	9.268(2)	2.713(2)	0.2927(2)	233.00(17)
2.95	9.261(1)	2.7124(8)	0.2929(1)	232.63(9)
3.06	9.256(2)	2.712(2)	0.2930(2)	232.31(16)
3.28	9.253(2)	2.712(2)	0.2931(2)	232.23(16)
3.40	9.254(1)	2.711(1)	0.2929(2)	232.13(11)
3.60	9.247(2)	2.710(2)	0.2931(2)	231.76(16)
4.28	9.237(2)	2.709(2)	0.2933(2)	231.15(16)
4.47	9.237(1)	2.706(2)	0.2930(3)	230.89(19)

rovskite (Liu, 1974). The variation of the structure with pressure, especially the effect of the substitution of Al for Si on the compression of the octahedron, will be of great crystal chemical interest. In this study, we have undertaken to measure the compressibility of the unit-cell and refine the structure at pressures up to 4.47 GPa.

Experimental

The single crystal used in this study was synthesized at approximately 1700 °C and 13 GPa (held for 2h) using a mix of K_2CO_3, Al_2O_3, and SiO_2 as starting material in a 2000-ton uniaxial split-sphere apparatus (USSA-2000) at the High-Pressure Laboratory of the State University of New York at Stony Brook. The crystal was chosen on the basis of optical examination and precession photographs. A subequant crystal 0.04 × 0.06 × 0.08 mm in size and a small piece of fluorite crystal were mounted in a diamond-anvil cell designed for single-crystal XRD studies (Hazen and Finger, 1982). The fluorite crystal was used as an internal standard of pressure following the method of Hazen and Finger (1981a); the estimated uncertainty in the cell pressure was ±0.1 GPa. An Inconel 750× gasket with a hole 0.40 mm in diameter was centered over one 0.60-mm diamond anvil; the crystal was then affixed to the anvil face inside the hole with a small dot of the alcohol-insoluble fraction of Vaseline petroleum jelly. A mixture of 4:1 methanol to ethanol was used as the hydrostatic pressure medium.

All X-ray measurements were performed with a Huber four-circle diffractometer with graphite monochromated Mo$K\alpha$ radiation (λ = 0.7093 Å). Unit-cell parameters were measured at 14 pressures. At each pressure, 7–12 reflections with 20° ≤ 2θ ≤ 38° were centered following the procedure of King and Finger (1979). Unit-cell parameters were initially refined as triclinic; at all pressures the unit-cell angles conform to the tetragonal dimensionality within 2 esd. Refined values of unit-cell parameters were determined using tetragonal constraints and are listed in Table 1. Whereas the unit-cell parameters at room conditions were somewhat different from those reported by Ringwood et al. (1967) (a = 9.38, c = 7.74 ± 0.01 Å), they were comparable to the results of Yamada et al. (1984) [a = 9.3244(4) Å, c = 2.7227(3) Å].

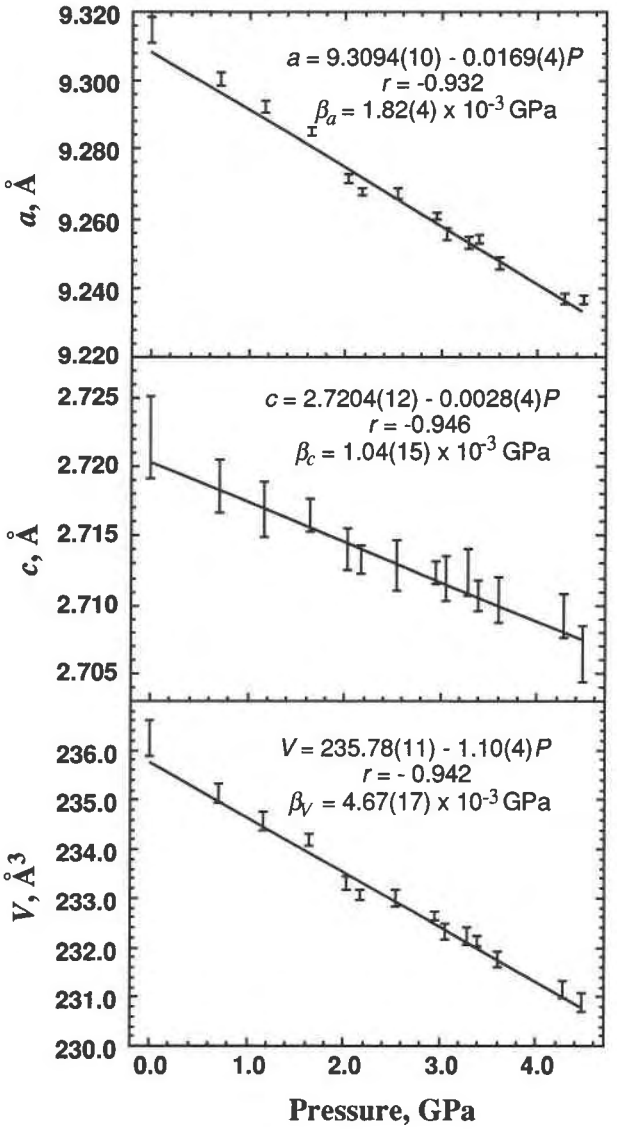

Fig. 1. Variations of unit-cell parameters with pressure.

Intensities were measured for all accessible reflections in a hemisphere of reciprocal space with $\sin(\theta/\lambda) \leq 0.7$. The fixed-$\phi$ mode of data measurement (Finger and King, 1978) was used to optimize reflection accessibility and minimize attenuation by the diamond cell. Corrections were made for Lorentz and polarization effects and for absorption by the diamond and Be components of the pressure cell. Omega step scans with step increments of 0.025° and 8-s counting time per step were used. Digitized step data were integrated by the method of Lehmann and Larsen (1974).

The structure of priderite (Sinclair and McLaughlin, 1982) was used as the initial model in the present work. The space group, *I*4/*m*, was assumed for the structure refinements. The scattering factor curves for K, Al, Si, and O are those of neutral atoms in *International Tables for X-ray Crystallography* (Ibers and Hamilton, 1974). Refinements were carried out with RFINE6 (Finger and

TABLE 2. Summary of refinement results

P (GPa)	$F \geq 2\sigma_F$	R^*	R_w^{**}
0	91	0.045	0.040
1.64	96	0.048	0.041
2.95	99	0.055	0.037
3.60	97	0.069	0.059
4.47	103	0.051	0.037

* $R = \Sigma||F_o| - |F_c||/\Sigma|F_o|$.
** $R_w = [\Sigma w(F_o - F_c)^2/\Sigma wF_o^2]^{0.5}$.

Prince, 1975) applying the robust-resistant weighting method of Prince et al. (1977). Crystal absorption and type 1 isotropic extinction corrections (Becker and Coppens, 1975) were made in the refinements.

RESULTS

Linear compressibilities and bulk modulus

Unit-cell parameters at 14 pressures, recorded in Table 1 and Figure 1, define the axial compressibilities of the crystal. The a axis is more compressible [$\beta_a = 1.82(4) \times 10^{-3}$/GPa] than the c axis [$\beta_c = 1.04(15) \times 10^{-3}$/GPa]. As in rutile-type compounds, **a** is approximately twice as compressible as **c** (Ross et al., 1990). Consequently, the c/a ratio increases with increasing pressure.

P-V data were fitted to a Birch-Murnaghan equation of state. The bulk modulus (K) is quite insensitive to the assumed pressure derivative (K_T'). For example, if V_0 is not constrained, the bulk modulus has the following values: 191(6) GPa at $K_T' = 4.0$; 187(6) GPa at $K_T' = 6.0$, the common K_T' value for rutile oxides (Ross et al., 1990); and 193(6) GPa at $K_T' = 2.8$, a K_T' reported by Ross et al. (1990) for stishovite. On the other hand, the calculated bulk modulus is sensitive to the constraint of V_0. Assuming K_T' to be 4.0 and including the constraint of V_0, the bulk modulus is 180(3), significantly smaller than the bulk modulus calculated without constraining V_0. As a recommended procedure (Jeanloz and Hazen, 1991), V_0 should be constrained in deriving equations of state from P-V data. Here, the value of 180(3) is reported as the bulk modulus of $KAlSi_3O_8$ hollandite. This bulk modulus is smaller than the bulk moduli of rutile-type oxides, which range from 212 to 313 GPa.

Structure refinements

The calculations for the structure refinements converged quickly to the R values listed in Table 2. The extinction coefficients, atomic coordinates, and isotropic displacement parameters are listed in Table 3. Bond distances, polyhedral volumes, distortion indices, O···O separations, and bond angles are summarized in Table 4. Tabulated observed and calculated structure factors are given in Table 5A–5E.[1]

[1] A copy of Table 5 may be ordered as Document AM-93-525 from the Business Office, Mineralogical Society of America, 1130 Seventeenth Street NW, Suite 330, Washington, DC 20036, U.S.A. Please remit $5.00 in advance for the microfiche.

TABLE 3. Positional and isotropic thermal parameters

	P (GPa)				
Parameter	0	1.64	2.95	3.60	4.47
Extinction coef. (10^{-4})	0.19(5)	0.16(5)	0.13(3)	0.15(6)	0.27(4)
K, x, y	0	0	0	0	0
z	½	½	½	½	½
B	1.18(8)	1.12(8)	0.98(8)	0.97(11)	0.95(7)
Si(Al), x	0.3501(3)	0.3501(3)	0.3503(3)	0.3507(4)	0.3503(3)
y	0.1661(3)	0.1658(3)	0.1659(3)	0.1662(4)	0.1662(3)
z	0	0	0	0	0
B	0.53(6)	0.43(6)	0.44(5)	0.41(8)	0.53(5)
O1, x	0.1526(7)	0.1532(7)	0.1542(6)	0.1546(9)	0.1541(7)
y	0.2036(7)	0.2036(6)	0.2035(6)	0.2030(9)	0.2027(7)
z	0	0	0	0	0
B	0.93(12)	0.76(12)	0.82(11)	0.87(15)	0.75(10)
O2, x	0.5406(6)	0.5411(6)	0.5400(5)	0.5401(8)	0.5406(5)
y	0.1648(6)	0.1659(6)	0.1651(6)	0.1651(9)	0.1623(6)
z	0	0	0	0	0
B	0.83(10)	0.58(10)	0.61(10)	0.60(14)	0.67(10)

DISCUSSION

The hollandite structure can be thought of as a rearranged rutile structure with open tunnels that accommodate large cations and H_2O molecules (Fig. 2a). The $Si(Al)O_6$ octahedra share edges to form double chains parallel to the **c** axis (Fig. 2b, 2c). These chains in turn share corners with neighboring double chains to form a framework structure. No ordering between Si and Al has been found in $KAlSi_3O_8$ hollandite, and Post and Burnham (1986) concluded that the octahedral cations in hollandite-type structures are probably disordered because of the narrow range of energies. The size of the $Si(Al)O_6$ octahedron determines the a and c axis lengths (Ringwood et al., 1967); c corresponds simply to the O1b···O1b and O2b···O2b distances in the octahedron.

It may be a coincidence that β_a and β_c of $KAlSi_3O_8$ hollandite are both 52.9% greater than β_a and β_c, respectively, of stishovite. The compressibility along **a** of $KAlSi_3O_8$ hollandite is close to the value $\beta_a = 1.80 \times 10^{-3}$/GPa for TiO_2 (Hazen and Finger, 1981b), but the compressibility of **c** is larger than any of the β_c values for the rutile-type compounds. As in stishovite, the difference in **a** and **c** axial compressibilities can be explained in large part by the stronger repulsive forces in the direction of **c** across the shared edge.

There are four unique bond distances in the distorted $Si(Al)O_6$ octahedron. For the convenience of description, the O atoms in the equatorial plane parallel to **c** are denoted as O1b and O2b, respectively, and the apical O atoms as O1a and O2a, respectively (Fig. 2b). Although O1a and O1b are symmetrically related, as are O2a and O2b, the Si(Al)-O1a and Si(Al)-O1b distances in one octahedron are different; also different are the Si(Al)-O2a and Si(Al)-O2b distances. In the octahedron shown in Figure 2b, the pyramid with apical O2a has no shared edges other than the basal O1b···O2b. The pyramid with apical O1a has two shared edges other than the basal O1b···O2b. Si(Al)-O1a is longer than Si(Al)-O2a, in-

TABLE 4. Polyhedral parameters, O···O separations, and bond angles at different pressures

Parameter	*P* (GPa)				
	0	1.64	2.95	3.60	4.47
			KO_8 polyhedron		
K-O1[8]*	2.733(5)	2.728(5)	2.726(4)	2.721(7)	2.713(5)
V (Å³)	30.58(7)	30.41(7)	30.34(6)	30.19(9)	29.90(7)
			Si(Al) octahedron		
Si(Al)-O1a	1.873(7)	1.862(7)	1.849(6)	1.844(9)	1.843(6)
Si(Al)-O1b[2]	1.825(5)	1.821(4)	1.817(4)	1.817(6)	1.816(4)
Si(Al)-O2a	1.774(6)	1.773(6)	1.757(6)	1.752(8)	1.759(5)
Si(Al)-O2b[2]	1.800(4)	1.791(4)	1.794(4)	1.793(5)	1.786(3)
Mean	1.816(5)	1.810(5)	1.805(5)	1.803(7)	1.801(4)
V (Å³)	7.86(3)	7.77(3)	7.70(2)	7.68(4)	7.65(3)
Quad. elon.	1.011(3)	1.011(3)	1.012(3)	1.012(3)	1.011(3)
Angle vari.	36.81	39.23	38.98	39.03	37.38
			O···O separation		
O1a···O2b[2]	2.428(10)	2.412(10)	2.393(9)	2.388(13)	2.395(9)
O1a···O2b[2]	2.655(8)	2.636(7)	2.633(7)	2.624(10)	2.636(6)
O1b···O2a[2]	2.568(8)	2.562(7)	2.561(7)	2.563(10)	2.573(6)
O1b···O2b[2]	2.386(8)	2.373(8)	2.377(7)	2.377(11)	2.372(7)
O2a···O2b[2]	2.618(7)	2.623(7)	2.605(6)	2.602(10)	2.570(6)
			Bond angle		
O1-K-O1[4]*	59.76(14)	59.72(12)	59.67(11)	59.73(17)	59.83(12)
O1-K-O1[8]	75.63(6)	75.65(5)	75.67(5)	75.64(8)	75.60(6)
O1-Si(Al)-O1[2]	82.1(3)	81.8(3)	81.5(2)	81.4(3)	81.8(2)
O1-Si(Al)-O2	169.7(3)	169.1(3)	169.4(3)	169.7(5)	170.7(3)
O1-Si(Al)-O2[2]	92.6(2)	92.3(2)	92.5(2)	92.3(3)	93.1(2)
O1-Si(Al)-O1	96.5(3)	96.5(3)	96.5(3)	96.4(4)	96.3(3)
O1-Si(Al)-O2[2]	91.1(3)	90.9(3)	91.5(2)	91.8(3)	92.1(2)
O1-Si(Al)-O2[2]	82.3(2)	82.2(2)	82.3(2)	82.4(3)	82.4(2)
O1-Si(Al)-O2[2]	174.7(3)	174.1(3)	174.0(3)	173.7(4)	174.9(3)
O2-Si(Al)-O2[2]	94.2(3)	94.8(3)	94.4(3)	94.4(5)	93.0(3)
O2-Si(Al)-O2	98.3(3)	98.6(3)	98.2(3)	98.2(4)	98.5(3)
Si(Al)-O1-Si(Al)[2]	97.9(3)	98.2(3)	98.5(2)	98.6(3)	98.3(2)
Si(Al)-O1-Si(Al)	96.5(3)	96.5(3)	96.5(3)	96.4(4)	96.3(3)
Si(Al)-O2-Si(Al)[2]	130.5(2)	130.3(2)	130.6(1)	130.6(2)	130.6(1)
Si(Al)-O2-Si(Al)	98.3(3)	98.6(3)	98.2(3)	98.2(4)	98.5(3)

* Bracketed figures represent multiplicity. The unit of length is ångström, and the unit of angle is degree.

creasing the cation to cation separations across shared edges. Also note that Si(Al)-O1b is slightly longer than Si(Al)-O2b.

Each octahedron has four shared edges, two O1b···O2b and two O1a···O1b. The shared edges are significantly shorter than the unshared ones. At room pressure, the unshared vertical edges are 2.723(4) Å, whereas the shared horizontal edges are 2.386(8) Å. Of the O···O separations, O1a···O1b and O2a···O2b (lying on the left front and right rear, respectively, of the octahedron in Fig. 2b) are the most compressible (Fig. 3). The relative incompressibility of the vertical O1b···O1b (or O2b···O2b) separation can be explained by the strong repulsive force between the Si(Al) atoms across the shared edge. The horizontal edges, O1b···O2b, are also incompressible because of their short length and the consequent strong repulsive force between the O^{2-} ions. Two other O···O separations, O1b···O2a and O1a···O2b, are less compressible because they are parallel to the plane of the double chain. Since O1a···O1b and O2a···O2b are more compressible, the net result of compression is a decrease in the dimension of the octahedron in the direction perpendicular to the plane of the double chain, i.e., the wall formed by the double-chain bands becomes thinner as the pressure increases.

The Si(Al)-O bond distances decrease linearly with increasing pressure (Fig. 4). The Si(Al)-O bond compressibilities are not determined by bond length alone. Although the longest Si(Al)-O1a bond is more compressible than the intermediate Si(Al)-O1b and Si(Al)-O2b bonds, the shortest Si(Al)-O2a bond is as compressible as Si(Al)-O1a. The larger compressibilities of the axial Si(Al)-O1a and Si(Al)-O2a bonds can be rationalized based on the thinning of the double-chain wall caused by the larger compressibilities of the O1a···O1b and O2a···O2b separations.

The following is a comparison of the $Si(Al)O_6$ octahedron in $KAlSi_3O_8$ and the SiO_6 octahedron in stishovite (data for the latter are results by Ross et al., 1990). The $Si(Al)O_6$ octahedron in $KAlSi_3O_8$ is slightly more distorted than the SiO_6 octahedron in stishovite. The difference between the longest and shortest Si(Al)-O bond distances in $KAlSi_3O_8$ is ~0.1 Å (Table 4), larger than the difference of ~0.05 Å in stishovite. At room pressure, the qua-

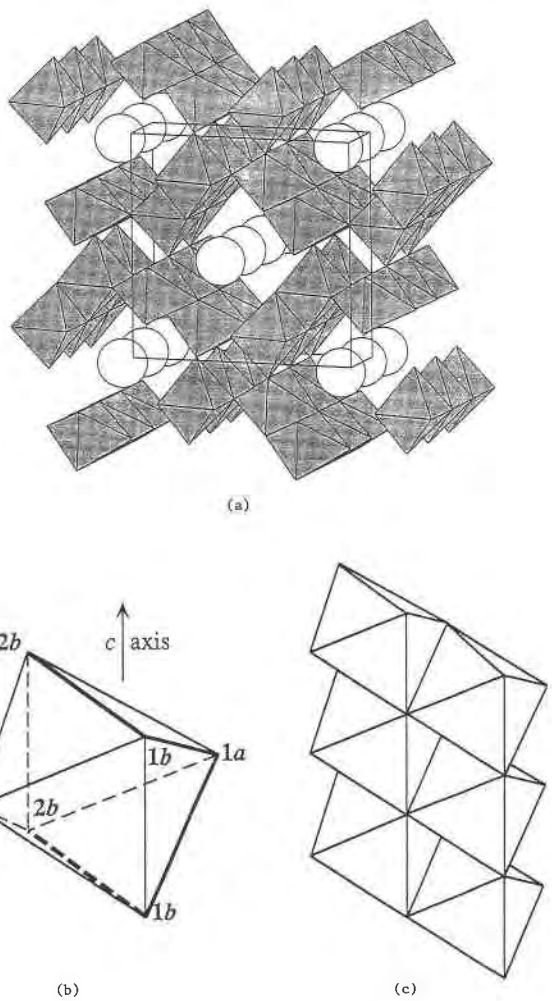

Fig. 2. (**a**) Structure of $KAlSi_3O_8$ hollandite, **c** perspective; open circles stand for K atoms. (**b**) Labeling of O atoms in the $Si(Al)O_6$ octahedron; coarse lines stand for shared edges. (**c**) Double chain formed by the octahedra.

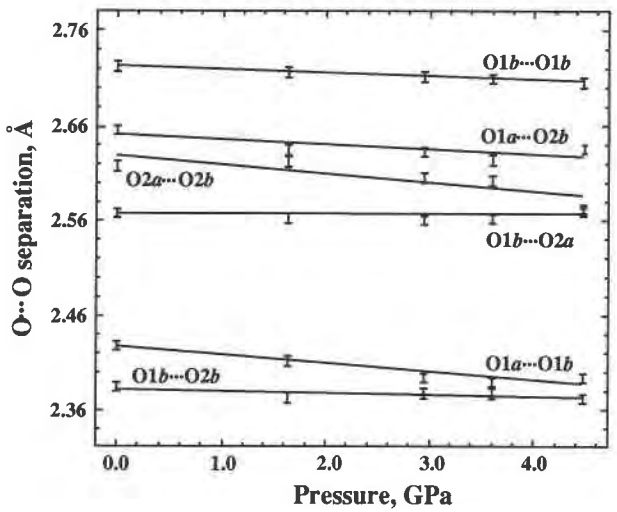

Fig. 3. Compressions of O···O separations.

dratic elongation and angle variance for the $Si(Al)O_6$ octahedron in $KAlSi_3O_8$ are 1.011(3) and 36.8, respectively, compared with 1.008 and 28.4 in stishovite. As in stishovite, no significant change in either distortion index is observed in $KAlSi_3O_8$ with increasing pressure. The angle O1b-Si(Al)-O2b subtended by the shared horizontal edge is 82.3(2)°, larger than the corresponding 81.3° angle in stishovite, probably owing to the weaker cation to cation repulsive force across the shared edge caused by the substitution of Al^{3+} for Si^{4+}. In this study, this angle did not show any change with increasing pressure, in agreement with the result of Ross et al. (1990) but contrary to the result of Sugiyama et al. (1987), who reported a slight decrease from 81.35° at room pressure to 80.1° at 6.09 GPa. The O1b-Si(Al)-O2a angle, however, increased from 91.1(3)° at room pressure to 92.1(2)° at 4.47 GPa. The shared horizontal edges of the $Si(Al)O_6$ octahedron [2.386(8) Å] are longer than the corresponding O···O separations in stishovite (2.29 Å) but still much shorter than twice the traditional ionic radius of O^{2-}, 2.64–2.80 Å (Shannon, 1976). As observed in stishovite, the axial bonds in $KAlSi_3O_8$ are approximately twice as compressible as the equatorial bonds.

The $Si(Al)O_6$ octahedron has a bulk modulus of 153(9) GPa, obtained by fitting a Birch-Murnaghan equation of state with $K_T' = 4.0$ to the pressure-polyhedral volume data (Fig. 5). The constraint of V_0 was not included for the reason that, unlike the unit-cell volume, V_0 of the octahedron was not well determined. The calculation of the polyhedral bulk modulus did not take into account the volume data error, which is large relative to the small volume of the (Si,Al) octahedron. As a consequence, the real error of the polyhedral bulk modulus should be larger than the error reported above. However, for all the rutile-type oxides, the polyhedral bulk moduli of the octahedra are generally equal to or slightly greater than the bulk moduli of the structures (Ross et al., 1990). With the assumption that $KAlSi_3O_8$ hollandite behaves in a similar manner, the polyhedral bulk modulus of the $Si(Al)O_6$ octahedron should be close to that of the structure, i.e., 180(3) GPa, which is still remarkably smaller than the value of 342 GPa by Ross et al. (1990) or the value of 250 GPa by Sugiyama et al. (1987) for the SiO_6 octahedron in stishovite. It is difficult to explain this unexpectedly small polyhedral bulk modulus by the substitution of Al for Si, since the AlO_6 octahedron in several structures has a common bulk modulus of ~220 GPa (Hazen and Finger, 1982). One explanation is that the calculated polyhedral bulk modulus is inaccurate and that the polyhedral bulk modulus is much larger than the bulk modulus of the structure. That is considered quite unlikely, on the basis that the unit-cell volumes of hollandite-related minerals are almost solely determined by the sizes

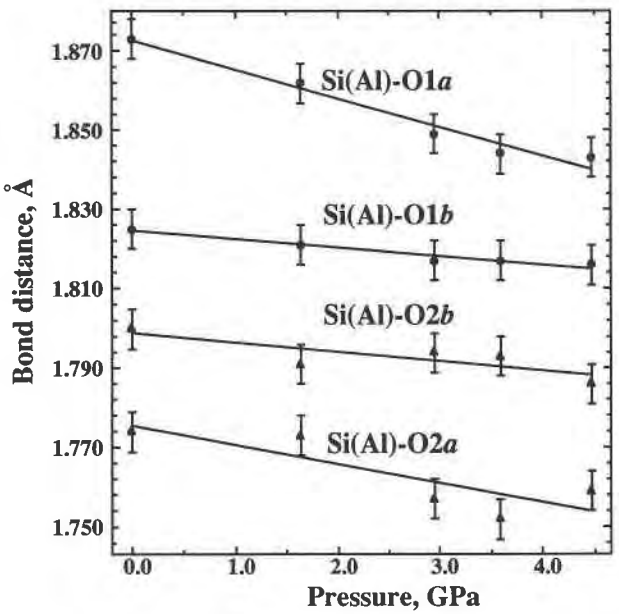

Fig. 4. Variations of Si(Al)-O bond distances with pressure.

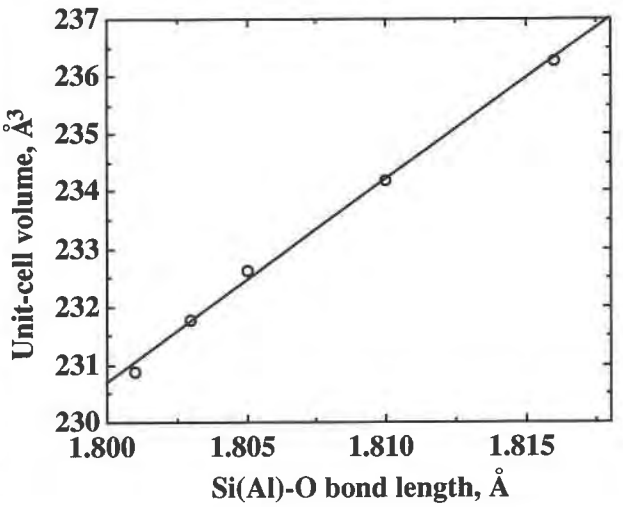

Fig. 6. Linear relationship between the unit-cell volume and the average octahedral bond distance.

of the octahedra (Ringwood et al., 1967; Post et al., 1982). An alternative explanation is that the substitution of Al for Si can greatly reduce the bulk moduli of the octahedron as well as that of the entire structure. The reason is not clear, but this explanation is supported by the drastic increase of 53% in the well-defined linear compressibilities of the crystal as a result of the replacement of ¼Si by Al.

As was observed by Ringwood et al. (1967) and Post et al. (1982), the unit-cell volume is linearly related to the average octahedral bond distance (Fig. 6). This would lead to the implication that the size of the unit-cell and, therefore, the sizes of the tunnel and the KO_8 polyhedron, are mainly determined by the Si(Al)-O framework and are quite independent of the size of the tunnel cation. The compressions of the two coordination polyhedra are compared in Figure 5. The polyhedral bulk modulus of the prism is 181(43) GPa, obtained by fitting a Birch-Murnaghan equation of state with $K_T' = 4.0$ and no constraint of V_0. This value is several times larger than that of the KO_6 polyhedron in phlogopite (27 GPa) and about twice that of CaO_8 in grossular (115 GPa) listed in Hazen and Finger (1982), in spite of the shorter Ca-O bond distance and the higher charge on Ca^{2+}. We conclude that

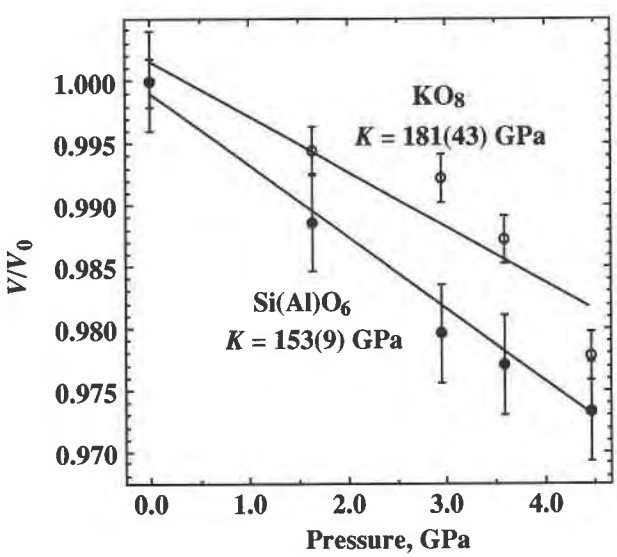

Fig. 5. Comparison of variations of V/V_0 with pressure for $Si(Al)O_6$ octahedron and KO_8 polyhedron.

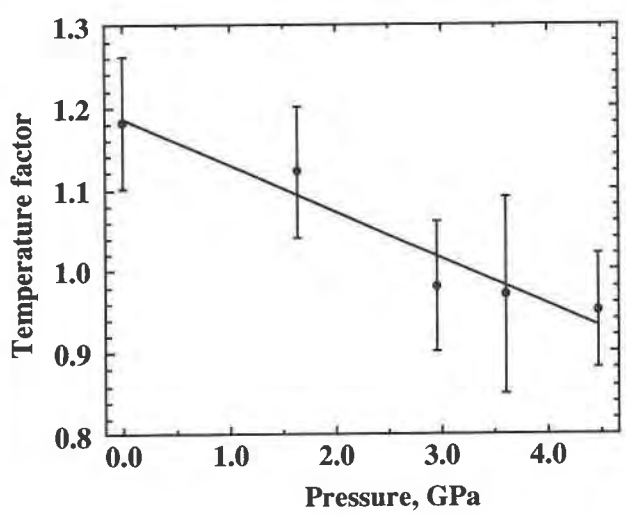

Fig. 7. Temperature factor of the K atom as a function of pressure.

the KO_8 polyhedron in $KAlSi_3O_8$ hollandite is not determined by its central cation and the coordinating anion but rather is constrained by the framework formed by the octahedra.

We observe an intriguing decrease of the isotropic temperature factor of the K atom with increasing pressure (Fig. 7). As the tunnel gets smaller, the thermal vibrations of K are more constrained. This trend serves as an indirect indication of good structure refinements.

Conclusions

In general, the response of the $KAlSi_3O_8$ hollandite structure is similar to that of the stishovite structure, with primary variations being the linear compression of cation to O bonds and O···O separations. As a first approximation, the shape of the unit cell and the atomic coordinates do not change with pressure. This is due to the constraint imposed by the tetragonal symmetry, which also causes the structure as well as the K site to compress at a rate similar to that of the $Si(Al)O_6$ octahedron. Consequently, the K-O_8 tetragonal prism has an apparent polyhedral bulk modulus unusually large for the K^+ cation. Compared with stishovite, the $KAlSi_3O_8$ hollandite structure, as well as its octahedral site, has an unexpectedly small bulk modulus. Since the octahedral site is so compressible, one would expect that it would not be able to sustain the compression at higher pressure, and a phase transformation would take place.

It would be of interest to subject $KAlSi_3O_8$ hollandite to higher pressure to test the possibility of a phase transformation—perhaps to the monoclinic form. In that eventuality the K polyhedron would be free to compress as the octahedral walls tilt. Consequently, such a high-pressure variant might be expected to display much greater compressibility than the tetragonal form. In this regard, it would also be of interest to study the variations of a hollandite structure with lower symmetry to find out if there is any clear distinction between the octahedral and tunnel-cation site compressibilities.

Acknowledgments

The synthesis of the $KAlSi_3O_8$ hollandite was performed in the Stony Brook High Pressure Laboratory, which is jointly supported by NSF Center for High-Pressure Research and the State University of New York. XRD work at the Geophysical Laboratory was supported by the NSF Center for High-Pressure Research, NSF grant EAR89-08192, and by the Carnegie Institution of Washington. We want to thank Charles W. Burnham (Harvard University) and Larry W. Finger (Geophysical Laboratory) for useful discussions.

References cited

Becker, P.J., and Coppens, P. (1975) Extinction within the limit of validity of the Darwin transfer equations. III. Non-spherical crystals and anisotropy of extinction. Acta Crystallographica, A31, 417–425.

Bish, D.L., and Post, J.E. (1989) Thermal behavior of complex, tunnel-structure manganese oxides. American Mineralogist, 74, 177–186.

Cheary, R.W., and Squadrito, R. (1989) A structural analysis of barium magnesium hollandites. Acta Crystallographica, B45, 1233–1246.

Finger, L.W., and Hazen, R.M. (1991) Crystal chemistry of six-coordinated silicon: A key to understanding the earth's deep interior. Acta Crystallographica, B47, 561–580.

Finger, L.W., and King, H.E. (1978) A revised method of operation of the single-crystal diamond cell and refinement of the structure of NaCl at 32 Kbar. American Mineralogist, 63, 337–342.

Finger, L.W., and Prince, E. (1975) A system of Fortran IV computer programs for crystal structure computations, 128 p. U.S. National Bureau of Standards Technical Note 854, Washington, DC.

Gruner, J.W. (1943) The chemical relationship of cryptomelane (psilomelane), hollandite, and coronadite. American Mineralogist, 28, 497–506.

Hazen, R.M., and Finger, L.W. (1981a) Calcium fluoride as an internal pressure standard in high pressure/high-temperature crystallography. Journal of Applied Crystallography, 14, 234–236.

——— (1981b) Bulk moduli and high-pressure crystal structures of rutile-type compounds. Journal of Physics and Chemistry of Solids, 42, 143–151.

——— (1982) Comparative crystal chemistry, 231 p. Wiley, New York.

Ibers, J.A., and Hamilton, W.C., Eds. (1974) International tables of X-ray crystallography, vol. IV, 366 p. Kynoch, Birmingham, U.K.

Jeanloz, R., and Hazen, R.M. (1991) Finite-strain analysis of relative compressibilities: Application to the high-pressure wadsleyite phase as an illustration. American Mineralogist, 76, 1765–1768.

King, H.E., and Finger, L.W. (1979) Diffracted beam crystal centering and its application to high-pressure crystallography. Journal of Applied Crystallography, 12, 374–378.

Lehmann, M.S., and Larsen, M.K. (1974) A method for location of the peaks in step-scan-measured Bragg reflections. Acta Crystallographica, A30, 580–584.

Liu, L. (1974) Silicate perovskite from phase transformation of pyrope-garnet at high pressure and temperature. Geophysical Research Letters, 1, 277–280.

Miura, H. (1987) The crystal structure of hollandite. Mineralogical Journal, 13, 119–129.

Post, J.E., and Burnham, C.W. (1986) Modelling tunnel-cation displacements in hollandites using structure-energy calculations. American Mineralogist, 71, 1178–1185.

Post, J.E., Von Dreele, R.B., and Buseck, P.R. (1982) Symmetry and cation displacement in hollandite: Structure refinements of hollandite, cryptomelane and priderite. Acta Crystallographica, B38, 1056–1065.

Prince, E., Nicholson, W.L., and Buchanan, J.A. (1977) A reanalysis of the data from the single crystal intensity project. American Crystallographic Association Programs and Abstracts, 5, 67.

Ringwood, A.E., and Major, A. (1971) Synthesis of majorite and other high pressure garnets and perovskites. Earth and Planetary Science Letters, 12, 411–418.

Ringwood, A.E., Reid, A.F., and Wadsley, A.D. (1967) High-pressure $KAlSi_3O_8$, an aluminosilicate with sixfold coordination. Acta Crystallographica, 23, 1093–1095.

Ringwood, A.E., Kesson, S.E., Ware, N.G., Hibberson, W., and Major, A. (1979) Immobilisation of high level nuclear reactor wastes in SYNROC. Nature, 278, 219–223.

Ross, N.L., Shu, J.F., and Hazen, R.M. (1990) High-pressure crystal chemistry of stishovite. American Mineralogist, 75, 739–747.

Shannon, R.D. (1976) Revised effective ionic radii and systematic studies of interatomic distances in halides and chalcogenides. Acta Crystallographica, A32, 751–767.

Sinclair, W., and McLaughlin, G.M. (1982) Structure refinement of priderite. Acta Crystallographica, B38, 245–246.

Sugiyama, M., Endo, S., and Koto, K. (1987) The crystal structure of stishovite under pressure up to 6 GPa. Mineralogical Journal, 13, 455–466.

Yamada, H., Matsui, Y., and Ito, E. (1984) Crystal-chemical characterization of $KAlSi_3O_8$ with the hollandite structure. Mineralogical Journal, 12, 29–34.

Manuscript received April 10, 1992
Manuscript accepted January 26, 1993